

A COASTAL OCEAN NUMERICAL MODEL

Alan F. Blumberg and George L. Mellor

Geophysical Fluid Dynamics Program

Princeton University

Princeton, NJ 08540

ABSTRACT

A coastal ocean model which, it is believed, is advanced beyond the current state of the art has been developed but is only in an early stage of application. Characteristics of the model include:

- * a second moment turbulence closure model capable of accurate prediction of small scale turbulent mixing and derivative ocean features such as mixed layer temperature and depth.
- * an algorithm which calculates the external (tidal) mode separately from the internal mode. The external mode, an essentially two-dimensional calculation, requires a short integrating time step whereas the costly, three-dimensional, internal mode can be executed with a long step. The result is a fully three-dimensional code which includes a free surface at no sacrifice in computer cost compared to rigid lid models.
- * a "σ" coordinate system with 20 levels in the vertical independent of depth. Thus, the environmentally important continental shelf, shelf bank and slope will be well resolved by the model. Furthermore, the model features increased resolution in the surface and bottom layers.
- * coding deliberately designed for modern array processing computers. This is essential to three-dimensional ocean simulations requiring long integrations at tolerable cost.

Reprinted from: Mathematical Modeling of Estuarine Physics, J. Sündermann and K.-P. Holz, Eds., Springer-Verlag Publishing Co., 203-219, 1980.

INTRODUCTION

In the last several years, second moment models of small scale turbulence have been developed at Princeton University (Mellor, 1973; Mellor and Durbin, 1975; Mellor and Yamada, 1974) such that mixing or the inhibition of mixing of momentum, temperature and salinity (or any other ocean property) can be predicted with considerable confidence. A number of other investigations have tested the simplest version of the model (Martin, 1976; Martin and Roberts, 1977; Weatherly and Martin, 1978) and it is now a part of the large, weather and climate General Circulation Models at NOAA's Geophysical Fluid Dynamics Laboratory (Miyakoda and Sirutis, 1977).

Incorporating an advanced version of this turbulence model (Mellor and Yamada, 1977), a three dimensional, time dependent, numerical ocean model has been recently constructed which, it is believed, is considerably advanced beyond that which is otherwise currently available. Mean velocity, temperature, salinity, turbulent kinetic energy and turbulent macroscale are prognostic variables. Free surface elevation is also calculated prognostically with no sacrifice in computational time. The model incorporates a " σ " coordinate system such that the number of grid points in the vertical is independent of depth. Furthermore, the spacing in this transformed coordinate system is also variable so that, for example, one may stipulate finer resolution near the surface and bottom layers resulting in an algorithm which will be very economical on modern array processing computers.

The model responds to tidal forcing, surface wind stress, heat flux, salt "flux" (i.e., evaporation minus precipitation), estuarine outflow and to the specification of temperature, salinity and sea surface elevation at open inflow boundaries.

At this writing, the model has just become operational. Some coastal ocean simulations are presented in this paper but the real effort of comparing data and calculation lies ahead.

DESCRIPTION OF THE NUMERICAL MODEL

Model Physics

The equations of motion which are solved by the model are:

$$\frac{\partial U}{\partial t} + \underline{V} \cdot \underline{\nabla} U - fV = - \frac{1}{\rho_0} \frac{\partial P}{\partial x} + \frac{\partial}{\partial z} \left[K_M \frac{\partial U}{\partial z} \right] + F_x \quad (1a)$$

$$\frac{\partial V}{\partial t} + \underline{V} \cdot \underline{\nabla} V + fU = - \frac{1}{\rho_0} \frac{\partial P}{\partial y} + \frac{\partial}{\partial z} \left[K_M \frac{\partial V}{\partial z} \right] + F_y \quad (1b)$$

$$0 = - \frac{\partial P}{\partial z} + \rho g \quad (2)$$

$$\frac{\partial U}{\partial x} + \frac{\partial V}{\partial y} + \frac{\partial W}{\partial z} = 0 \quad (3)$$

$$\frac{\partial T}{\partial t} + \underline{V} \cdot \underline{\nabla} T = \frac{\partial}{\partial z} \left[K_H \frac{\partial T}{\partial z} \right] + F_T \quad (4)$$

$$\frac{\partial S}{\partial t} + \underline{V} \cdot \underline{\nabla} S = \frac{\partial}{\partial z} \left[K_H \frac{\partial S}{\partial z} \right] + F_S \quad (5)$$

where U, V, T, S are the mean velocity components, temperature and salinity and we define $\underline{V} \cdot \underline{\nabla}(\) \equiv U\partial(\)/\partial x + V\partial(\)/\partial y + W\partial(\)/\partial z$. The turbulence field is characterized by

$$\frac{\partial q^2}{\partial t} + \underline{V} \cdot \underline{\nabla} q^2 = \frac{\partial}{\partial z} \left[K_q \frac{\partial q^2}{\partial z} \right] + 2(P_s + P_b) - 2\epsilon + F_q \quad (6)$$

$$\frac{\partial}{\partial t} (q^2 \ell) + \underline{V} \cdot \underline{\nabla} (q^2 \ell) = \frac{\partial}{\partial z} \left[K_q \frac{\partial}{\partial z} (q^2 \ell) \right] + \ell E_1 (P_s + E_3 P_b) - \ell \epsilon \widetilde{W} + F_\ell \quad (7)$$

where $q^2/2$ is the turbulent kinetic energy; ℓ is a turbulent macroscale; P_s and P_b are turbulent shear and buoyancy production; ϵ is dissipation and \widetilde{W} is a wall proximity function. The problem is primarily closed by expressions for $K_M, K_H,$ and K_q

which are function of $\partial U/\partial z$, $\partial V/\partial z$, $\rho_0^{-1} g\partial\rho/\partial z$, ℓ and q . These are analytically derived relations emanating from closure hypotheses described and implemented by Mellor (1973), Mellor and Yamada (1974), Yamada and Mellor (1975) and most recently by Mellor and Yamada (1977). Appendix A contains most of the details. Empirical constants in these algebraic relations are derived from neutral data but the result has been shown to predict the stabilizing or destabilizing effects of density stratification. The density, ρ , is of course related to temperature and salinity through an equation of state for sea water.

The terms, F_x , F_y , F_T , F_S , F_q and F_ℓ represent horizontal diffusion which are usually required by models to damp small scale numerical computational modes. Oftentimes, the required horizontal diffusivities give rise to excessive smoothing of real oceanographic features. The problem is, of course, ameliorated by decreasing horizontal grid size. In our case, we believe that relatively fine *vertical* resolution results in a reduced need for *horizontal* diffusion; i.e., horizontal advection followed by vertical mixing effectively acts as horizontal diffusion in a real physical sense.

Boundary Conditions

The boundary conditions at the free surface, $z = \eta(x,y)$, are:

$$K_M \left(\frac{\partial U}{\partial z}, \frac{\partial V}{\partial z} \right) \sim (\tau_{ox}, \tau_{oy}) \text{ as } z \rightarrow \eta \quad (8a,b)$$

$$K_H \left(\frac{\partial T}{\partial z}, \frac{\partial S}{\partial z} \right) \sim (\dot{H}, \dot{S}) \text{ as } z \rightarrow \eta \quad (9a,b)$$

$$q^2 = B_1 u_\tau^2, \quad z = \eta \quad (10)$$

$$q^2 \ell = 0, \quad z = \eta \quad (11)$$

$$W = U \frac{\partial \eta}{\partial x} + V \frac{\partial \eta}{\partial y} + \frac{\partial \eta}{\partial t}, \quad z = \eta \quad (12)$$

where (τ_{ox}, τ_{oy}) is the surface wind stress vector, \dot{H} is the net ocean heat flux and $\dot{S} = S(0)[\dot{E}-\dot{P}]/\rho_0$ where $(\dot{E}-\dot{P})$ is the net evaporation-precipitation fresh water surface flux rate. In equation (10), $u_\tau^2 = |\underline{\tau}_0|$ and B_1 is one of the empirical constants in the turbulent closure relations.

At the bottom, $z = -H(x,y)$, boundary conditions for T , S , q^2 and $q^2 \ell$ are similar to

(9a,b), (10) and (11) where, however, $\dot{H} = \dot{S} = 0$. In place of (12) we have $W = -U\partial H/\partial x - V\partial H/\partial y$ where $H(x,y)$ is the bottom topography. Bottom boundary conditions for U and V are supplied by matching the solution to the logarithmic law of the wall which requires a bottom roughness parameter. In deep water, bottom boundary layers may be unimportant, but may assume some importance on the shelf. However, some recent work by Armi (1978) indicates that bottom boundary layers are important for the long time scale development of the thermocline. The hypothesis is that bottom boundaries on, say the continental slopes, mix adjacent vertical layers of water which are then advected into the interior. According to the hypothesis this effect may be more important than small vertical mixing attributable to internal gravity wave breaking, at least, in deeper water well below the mixed layer. Our model, in principle, can account for this behavior.

In the Middle Atlantic Bight simulation discussed later, open boundary conditions require temperature and salinity. Geostrophically derived, vertical gradients of horizontal velocity may be calculated but then either total transport or sea surface elevation is also required.

Numerical Scheme

To achieve computational economy the program is divided into external and internal mode subprograms. The first, call it the XYt subprogram, computes the vertically averaged velocity and the surface elevation fields with a short time increment (≈ 30 sec.) imposed by the shallow water wave speed, CFL criterion, The second, call it the XYZT subprogram, computes the full three-dimensional velocity, temperature and salinity fields with a much longer time increment (≈ 40 minutes). The XYZT subprogram incorporates the second moment turbulent closure model. It supplies computed bottom friction and vertical integrals of density and vertical variances of horizontal velocity to the XYt subprogram where they behave as lateral friction-like terms in the vertically averaged horizontal equations of motion. (These terms must be parameterized by horizontal eddy viscosities in models which do not adequately resolve vertical structure.) In turn, the XYt subprogram supplies sea surface evaluation to the XYZT subprogram. This may sound complicated, but in the final analysis, the full, three-dimensional field equations are solved with a free surface boundary condition at no additional cost in computer time as compared to rigid lid models (Bryan and Cox, 1968).

The time differencing is the conventional leap frog technique. However, the scheme is quasi-implicit in that vertical diffusion is evaluated at the forward time level. Thus, small vertical spacing is permissible near the surface without need to reduce the time increment or restrict the magnitude of the mixing coefficients.

The vertical coordinate is scaled such that $\sigma = (z-\eta)/(H+\eta)$ and all equations are transformed to x, y, σ, t . Currently, we use 20 vertical levels with increasingly fine resolution near the surface and bottom so that surface and bottom mixed layers are resolved. The resolution in physical space increases shoreward as H decreases.

Present Status of the Model

In the process of developing the model some intrinsically interesting exploratory calculations have been made. The initial numerical experiments involve the 2-D, XYt mode (all longshore gradients are neglected) to simulate the effects of coastal upwelling and downwelling. Figures 1, 2 and 3 illustrate the results of an impulsively imposed alongshore wind stress. Three cases are considered: Figure 1 is a homogeneous, upwelling event, Figure 2 a density stratified, upwelling event, and Figure 3 is a density stratified, downwelling event. The role of stratification in confining mixing to surface and bottom layers is readily apparent. In Figure 2 one will observe the formation of a near shore ($x = 2\text{km}$) baroclinic jet.

The numerical code has also been exercised in the external (tidal) mode. An application of this mode to the Chesapeake Bay (Blumberg, 1977) showed considerable success. The 2-D tidal mode also has been applied to the Middle Atlantic Bight ($1/4^\circ$ horizontal resolution). Figure 4 illustrates the dynamic response of a "barotropic" MAB to various surface elevation boundary conditions imposed along the open portions of the domain.

The fully three-dimensional code has only very recently become operational with two time steps (recall that the external, vertically averaged mode requires a short time step, whereas the fully three-dimensional calculations can be executed with an economically long time step) after a long debugging period. Figure 5 is the result of a calculation of the Middle Atlantic Bight circulation with manufactured temperature and salinity distributions for initialization and for open boundary conditions. The normal component of velocity along the open boundary is specified by geostrophic balance with a level of no motion at the bottom. Also, for this calculation the surface wind stress and fluxes are zero. A transect east of Cape Hatteras is shown in Figure 6; contours of north/south velocity are drawn in this diagram.

Numerical experiments are now being conducted using the climatological temperature and salinity distributions described by Blumberg, Mellor and Levitus (1978) as initial conditions and at the open boundaries. Preliminary prognostic simulations (temperature, salinity and therefore density are simulated) show a broad, slow Gulf Stream together with a southward flow along the coast. The velocity distributions spin-up in about 5 days; however, the temperature and salinity fields evolve more slowly.

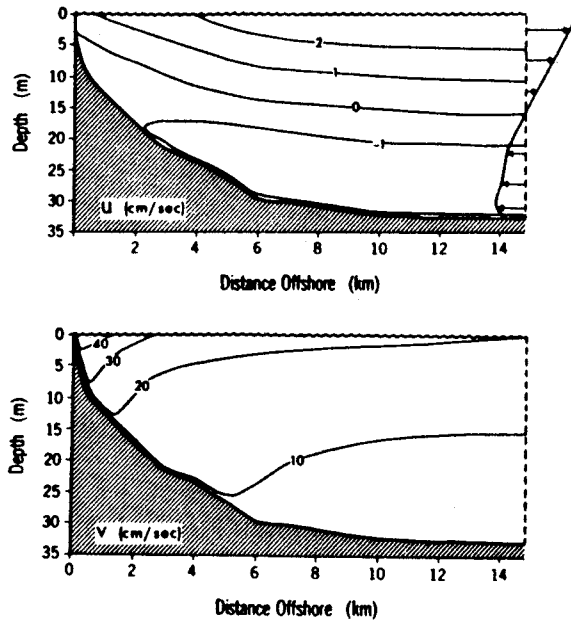


Figure 1. A homogeneous upwelling event induced by an alongshore wind stress of 2.0 dynes/cm^2 directed into the plane of the paper. The wind stress has been imposed for six hours. The onshore (U negative) and offshore (U positive) isotachs are depicted in the upper portion of the figure, while the alongshore (V positive into the plane of the paper and V negative out of the plane of the paper) isotachs are depicted in the lower portion.

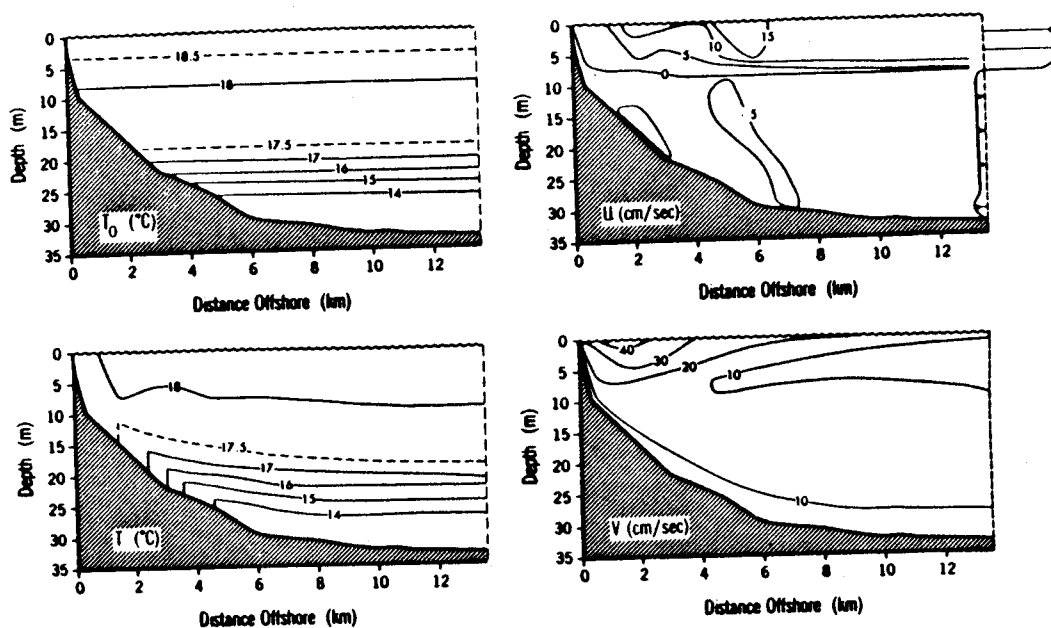


Figure 2. A stratified upwelling event induced by an alongshore wind stress of 1.0 dyne/cm directed into the plane of the paper. This wind stress has been imposed for twelve hours. The direction of the isotachs is the same as in figure 1. The initial temperature distribution is denoted as T_0 .

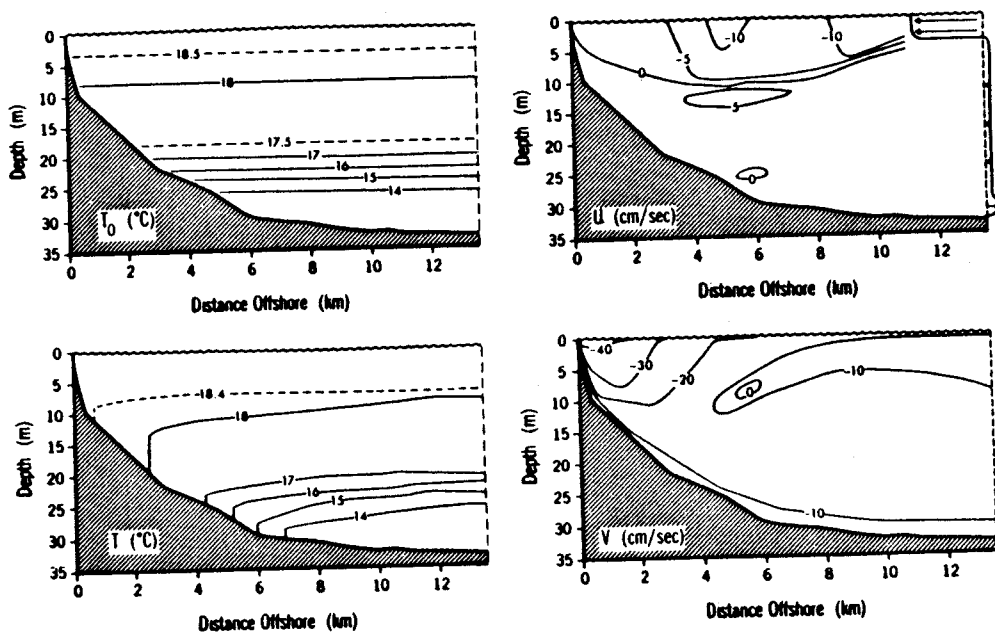
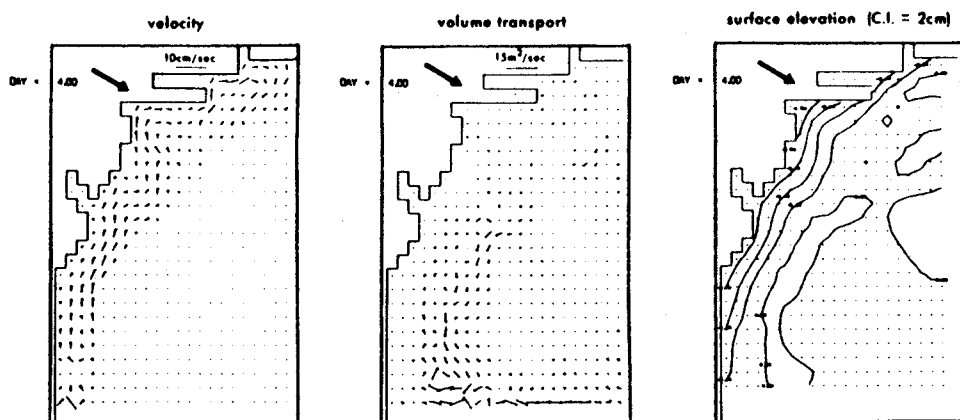
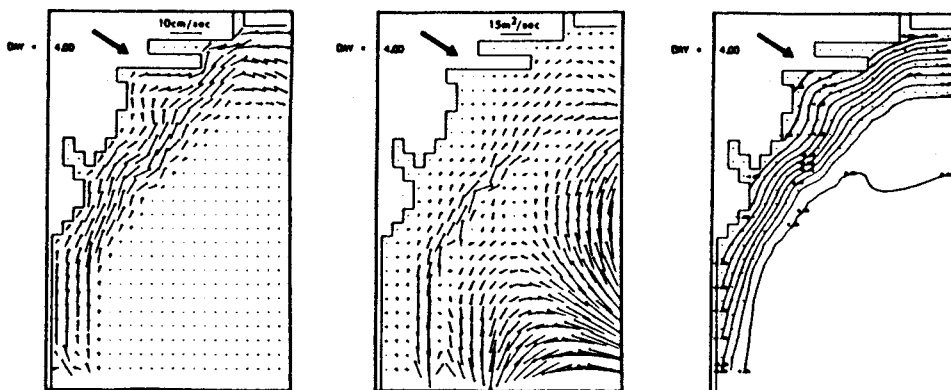


Figure 3. A stratified downwelling event induced by an alongshore wind stress of 1.0 dyne/cm² directed out of the plane of the paper. The wind stress has been imposed for twelve hours. The direction of the isotachs is the same as in figure 1. The initial temperature distribution is denoted as T_0 .



Case A: Zero surface elevation along open boundary



Case B: Modified radiation condition at open boundary

Figure 4. A comparison of the dynamic response of the Middle Atlantic Bight after four days to various surface elevation boundary conditions. The heavy arrow indicates the direction of the 1.2 dyne/cm² wind stress imposed at Day=0.

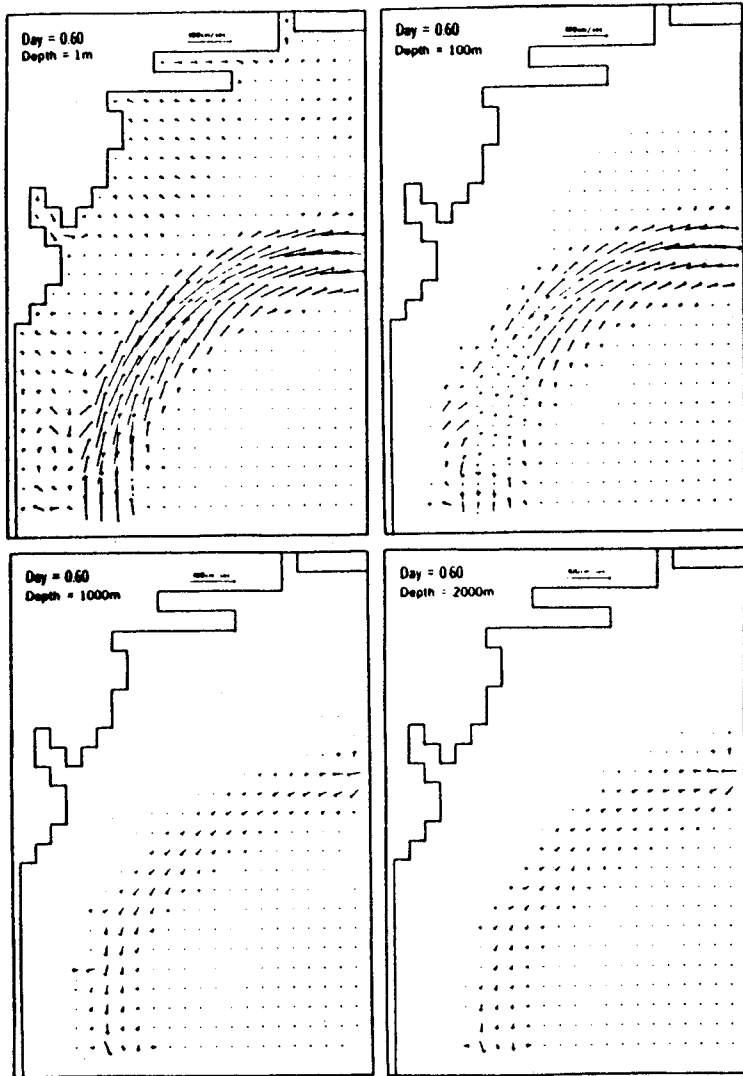


Figure 5. Density driven circulation patterns in the MAB at various depths for a manufactured temperature and salinity distribution.

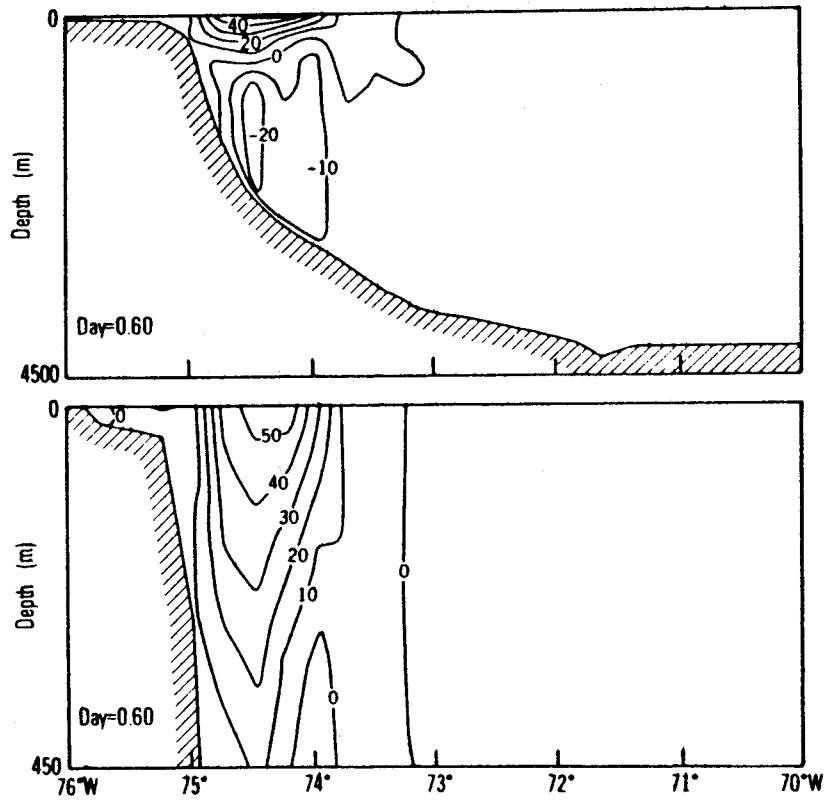


Figure 6. Contours of calculated North/South velocity (isotachs in cm/sec) on Latitude 36°N. The lower figure is a detail of the upper 450m.

CONCLUSION

The construction and implementation of a fully three-dimensional numerical model capable of predicting the dynamics and thermodynamics of coastal ocean regions is presented. Genuine simulations for comparison with real data have yet to be initiated and will, in fact, be the major goal of future research.

ACKNOWLEDGMENTS

This work is a result of research sponsored by NOAA Office of Sea Grant, Department of Commerce, under Grant # 04-6-158-4476, and NOAA/Princeton University, Visiting Scientist Grant # 04-7-022-4417.

APPENDIX A

Since the paper by Mellor and Yamada (1974), a few modifications have been made to the boundary layer model.

First, the "Level 3" model was further simplified into a "Level 2 1/2" model by neglect of the material and diffusive derivatives for scalar (temperature, salinity, density, etc.) variances. The loss in predictive accuracy is not expected to be important (Yamada, 1977).

Second, as discussed by Mellor and Yamada (1977), the empirical constants cited below have been changed slightly from the original values after a critical reexamination of the data upon which they are based. The overall effect of these changes should be quite small indeed.

A third modification is incorporated here and results from trials of a suggestion by Rodi (1972). Consider the model equations for $\overline{u_i u_j}$, $\overline{u_i \rho'}$ and $\overline{\rho'^2}$:

$$\begin{aligned} \mathcal{L}_1(\overline{u_i u_j}) = & -\overline{u_k u_i} \frac{\partial u_j}{\partial x_k} - \overline{u_k u_j} \frac{\partial u_i}{\partial x_k} - \frac{2}{3} \frac{q^3}{\Lambda_1} \delta_{ij} \\ & + g_j \overline{u_i \rho'} + g_i \overline{u_j \rho'} \\ & - \frac{q}{3\ell_1} (\overline{u_i u_j} - \frac{\delta_{ij}}{3} q^2) + C_1 q^2 \left(\frac{\partial u_i}{\partial x_j} + \frac{\partial u_j}{\partial x_i} \right) \end{aligned} \quad (A1)$$

$$\mathcal{L}_2(\overline{u_j \rho'}) = -\overline{u_k u_j} \frac{\partial \bar{\rho}}{\partial x_k} - \overline{\rho' u_k} \frac{\partial u_j}{\partial x_k} - g_i \overline{\rho'^2} + \frac{q}{3\ell_2} \overline{u_i \rho'} \quad (A2)$$

$$0 = \overline{u_k \rho'} \frac{\partial \bar{\rho}}{\partial x_k} - \frac{q}{3\ell_2} \overline{\rho'^2} \quad (A3)$$

the operators $\mathcal{L}_1(\)$ and $\mathcal{L}_2(\)$ represent the material and diffusive derivative terms. The corresponding terms in (A3) have been neglected in accordance with our previous comments.

Now (A1) upon contraction yields the turbulent energy equation,

$$\mathcal{L}_3(q^2) = 2(P_s + P_b - \epsilon) \quad (A4)$$

where, if $g_i = (0, 0, -g)$, production and dissipation are defined according to

$$P_s \equiv - \overline{u_i u_j} \frac{\partial u_i}{\partial x_j}, P_b = - g \overline{w \rho'}, \epsilon \equiv \frac{q}{\Lambda_1}^3 \quad (\text{A5a,b,c})$$

and $\mathcal{L}_3(\)$ is very nearly but not exactly identical to $\mathcal{L}_1(\)$. Rodi's suggestion is to replace $\mathcal{L}_1(\overline{u_i u_j})$ in (A1) with $(\overline{u_i u_j}/q^2) \mathcal{L}_3(q^2)$, where $\mathcal{L}_3(q^2)$ is obtained in (A4). This could have been incorporated into the paper of Mellor and Yamada (1974) as an alternative and apparently equally consistent step by replacing $\delta_{ij}/3$ by $\overline{u_i u_j}/q^2$ at one point in their analysis.¹ Note that if we define a_{ij} such that $\overline{u_i u_j} = (\delta_{ij}/3 + a_{ij})q^2$ then $a_{ij} \rightarrow 0$ defines an isotropic limit. Thus, incorporation of Rodi's idea introduces a higher order term into the Mellor-Yamada analysis. This is not incorrect but is somewhat arbitrary since other terms, presumably of the same order, have been neglected. The choice has been made here on the basis that the resulting algorithm survives numerical trauma better than its predecessor and in the hope that the resulting approximation is closer to the full (level 4) equation set.

A similar step is to replace $\mathcal{L}_2(\overline{u_i \rho'})$ with $(\overline{u_i \rho'}/2 q^2) \mathcal{L}_3(q^2)$ since a term like $\mathcal{L}(\overline{\rho'^2})$ on the left of (A3) has already been neglected.

The result of these substitutions is that (A1) and (A2) may be rewritten as

$$\begin{aligned} 2 \frac{\overline{u_i u_j}}{q^2} (P_s + P_b - \epsilon) &= - \overline{u_k u_i} \frac{\partial u_j}{\partial x_k} - \overline{u_k u_j} \frac{\partial u_i}{\partial x_k} - \frac{2}{3} \delta_{ij} \\ &+ g_i \overline{u_j \rho'} + g_j \overline{u_i \rho'} \\ &- \frac{q}{3\ell_1} (\overline{u_i u_j} - \frac{\delta_{ij}}{3} q^2) + \overline{c_1} q^2 (\frac{\partial u_i}{\partial x_j} + \frac{\partial u_j}{\partial x_i}) \end{aligned} \quad (\text{A6})$$

$$\begin{aligned} \frac{\overline{u_i \rho'}}{q} (P_s + P_b - \epsilon) &= - \overline{u_j u_k} \frac{\partial \overline{\rho}}{\partial x_k} - \overline{\rho' u_k} \frac{\partial u_i}{\partial x_k} - \frac{q}{3\ell_2} \overline{u_i \rho'} \\ &- g_j \frac{\Lambda_2}{q} \overline{u_k \rho'} \frac{\partial \overline{\rho}}{\partial x_k} \end{aligned} \quad (\text{A7})$$

where $\overline{\rho'^2}$ in (A2) has been replaced using (A3).

Now, if one makes the boundary layer approximation in (A6) and (A7), all components

¹Thus on page 1793 of the Mellor-Yamada paper, in the first sentence below equation (8), substitute $\overline{u_i u_j}/q^2$ in place of $\delta_{ij}/3$.

of the tensor, $\partial U_j / \partial x_k$, may be neglected except for $\partial U / \partial z$ and $\partial V / \partial z$. Then, if we again set $g_i = (0, 0, -g)$, and define $-\overline{(uw)}, \overline{(vw)} = K_M (\partial U / \partial z, \partial V / \partial z)$ and $-\overline{\rho'w} = K_H \partial \rho / \partial z$, and furthermore define

$$K_m \equiv \ell q S_M, \quad K_H \equiv \ell q S_H \quad (\text{A8a,b})$$

and

$$\phi_1 \equiv 1 + \frac{3\ell_1}{q^3} (P_s + P_b - \epsilon) = 1 + \frac{3\ell_1}{\Lambda_1} \left(\frac{P_s + P_b}{\epsilon} - 1 \right) \quad (\text{A9a})$$

$$\phi_2 \equiv 1 + \frac{3\ell_2}{q^3} (P_s + P_b - \epsilon) = 1 + \frac{3\ell_2}{\Lambda_1} \left(\frac{P_s + P_b}{\epsilon} - 1 \right) \quad (\text{A9b})$$

$$C_1 \equiv \frac{\widetilde{C}_1}{\phi_1} \quad (\text{A9c})$$

$$G_H \equiv \frac{\ell^2}{q^2} \frac{g}{\rho_o} \frac{\partial \overline{\rho}}{\partial z} \quad (\text{A9d})$$

then

$$\begin{aligned} S_M \left[\phi_1 - \frac{9A_1 A_2 G_H}{\phi_2} \right] - S_H \left[\frac{18A_1^2 G_H}{\phi_1} + \frac{9A_1 A_2 G_H}{\phi_2} \right] \\ = A_1 \left[\frac{1 - 6A_1/B_1 - 3C_1}{\phi_1} \right] \end{aligned} \quad (\text{A10})$$

$$S_H \left[\phi_1 - 3A_2 B_2 G_H - 18A_1 A_2 G_H \right] = A_2 \left[\frac{1 - 6A_1/B_1}{\phi_1} \right] \quad (\text{A11})$$

Equation (A9c) where $C_1 = \text{constant}$ is another numerically motivated modification and has no physical basis. Generally $\widetilde{C}_1 \approx C_1$ except in start up situations or below the mixed layer where q^2 and other variables are dominated by round-off error.

It may be shown that the correlation equations for temperature and salinity are identical to those for density so that

$$-\overline{wT'} = K_H \partial T / \partial z \quad \text{and} \quad -\overline{wS'} = K_H \partial S / \partial z.$$

Thus the algebraic forms of (A10) and (A11) have been altered somewhat from the original Level 3 model of Mellor and Yamada (1974, 1977). For $P_s + P_b = \epsilon$, the model collapses to the same Level 2 (e.g., as in Mellor and Durbin, 1975) model as before. In fact, the present version conforms very nearly to the previous version when $0 < (P_s + P_b) / \epsilon < 2$ but is numerically more rugged and more readily accommodates start-up shocks, for example.

A necessary assumption is that all lengths are proportional to each other. Thus, we let

$$(\ell_1, \ell_2, \Lambda_1, \Lambda_2) = (A_1, A_2, B_1, B_2)\ell \quad (\text{A12})$$

By appealing to simple laboratory data (Mellor and Yamada, 1977) all of the empirical constants were assigned the values;

$$(A_1, A_2, B_1, B_2, C_1) = (.92, .74, 16.6, 10.1, 0.08) \quad (\text{A13})$$

There remain unknowns in equations (6) and (7). First, in analogy to (A8a,b) we define

$$K_q \equiv \ell q S_q \quad (\text{A14})$$

Since we have found that S_M and S_H are dependent on stability, one would suppose this to be the case with S_q , although a determination of S_q similar to that of S_M and S_H would require an appeal to equations for triple correlations which would require additional modelling assumptions and constants. Thus we have variously tried $S_q = \text{constant} = 0.20$ (determined from neutral boundary layer and channel flow data) and the stability dependent $S_q = 0.20(S_M/0.392)$ where the value $S_M = 0.392$ corresponds to neutral flow and where production is balanced by dissipation. However, results are not overly sensitive to this choice. In this paper, we have used the second prescription for S_q .

In equation (7), \widetilde{W} is a "wall proximity" function defined as

$$\widetilde{W} = 1 + E_2 \left(\frac{\ell}{L}\right)^2 \quad (\text{A15})$$

L has a more general definition but for the ocean problem $(\kappa L)^{-1} = (n-z)^{-1} + (H+z)^{-1}$. Near surfaces it may be shown that both ℓ and L are proportional to distance from the surface ($\kappa=0.4$ is the constant of proportionality) and therefore $\widetilde{W} = 1 + E_2$; far from surfaces $\widetilde{W} = 1$.

Finally, the following constants have been determined from simple laboratory boundary layer and channel flow data (Mellor and Yamada, 1977) such that

$$(E_1, E_2, E_3) = (1.8, 1.33, 1.0) \quad (\text{A16})$$

$E_3 = 1.0$ is a default value awaiting a comparison of a data set and calculation that would discriminate an alternative value.

REFERENCES

- Armi, L., 1978: Some evidence for boundary mixing in the deep ocean. *J. Geoph. Res.*, 83, 1971-1979.
- Blumberg, A., 1977: Numerical tidal model of Chesapeake Bay. *J. of the Hydraulic Division.*, ASCE, 103, (HY1), 1-10.
- Blumberg, A.F., G.L. Mellor, and S. Levitus., 1977: The Middle Atlantic Bight: A climatological atlas of oceanographic properties. Princeton University Sea Grant Report No. NJ/P-SG-01-8-77.
- Bryan, K., and M.D. Cox., 1968: A nonlinear model of an ocean driven by wind and differential heating. Parts I and II. *J. Atmos. Sci.*, 25, 945-978.
- Martin, P.J. 1976: A comparison of three diffusion models of the upper mixed layer of the ocean. NRL-GFD/OTEC 4-76, 1-56.
- Martin, P.J. and G.O. Roberts. 1977: An estimate of the impact of OTEC operation on the vertical distributions of heat in the Gulf of Mexico. Proceeding, Fourth Annual Conference on Ocean Thermal Energy Conversion, New Orleans.
- Mellor, G.L., 1973: Analytic prediction of the properties of stratified planetary surface layers. *J. Atmos. Sci.*, 30, 1061-1069.
- Mellor, G.L. and T. Yamada., 1974: A hierarchy of turbulence closure models for planetary boundary layers. *J. Atmos. Sci.*, 31, 1791-1806.
- Mellor, G.L. and P.A. Durbin, 1975: The structure and dynamics of the ocean surface mixed layer., *J. Phys. Oceanogr.*, 5, 718-728.
- Mellor, G.L. and T. Yamada, 1977: A turbulence model applied to geophysical fluid problems. Proceedings: Symposium on Turbulent Shear Flows, Pennsylvania State University, University Park, Pennsylvania, April 1977, 1-14.
- Miyakoda, K. and J. Sirutis, 1977: Comparative integrations of global models with various parameterized processes of subgrid-scale vertical transports: Description of the parameterizations. *Beitrag zur Physik der Atmosphere.*, 50, 445-487.
- Rodi, W., 1972: The prediction of free turbulent boundary layers by use of a 2-equation model of turbulence. Ph.D. thesis, University of London.
- Weatherly, G. and P.J. Martin., 1978: On the structure and dynamics of the oceanic bottom boundary layer. *J. Phys. Oceanogr.*, 8, 557-570.
- Yamada, T. and G.L. Mellor., 1975: A simulation of the Wangara atmospheric boundary layer data., *J. Atmos. Sci.*, 32, 2309-2329.
- Yamada, T., 1977: A numerical experiment on pollutant dispersion in a horizontally-homogeneous atmospheric boundary layer., *Atmosphere Environment.*, 11, 1015-1024.